Coupling of a regional atmospheric model (RegCM3) and a regional oceanic model (FVCOM) over the maritime continent

Coupling of A Regional Atmospheric Model (RegCM3) and A Regional Oceanic Model (FVCOM) Over the Maritime Continent

Jun Wei[1,2]; Dongfeng Zhang[2]; Paola Malanotte-Rizzoli[2,3]; and Elfatih A B Eltahir[2,3]

1: Peking University, Beijing, China

2: Singapore-MIT Alliance for Research and Technology, Singapore

3: Massachusetts Institute of Technology, Cambridge, MA, USA

*Corresponding Author: Jun Wei (junwei@pku.edu.cn)

Abstract

We describe a successful coupling of two regional models of the atmosphere and the ocean: Regional Climate Model version 3 (RegCM3) and Finite Volume Coastal Ocean Model (FVCOM). RegCM3 includes several options for representing important processes such as moist convection and land surface physics. FVCOM features a flexible unstructured grid that can match complex land and islands geometries as well as the associated complex topography. The coupled model is developed and tested over the Southeast Asian Maritime Continent, a region where a relatively shallow ocean occupies a significant fraction of the area and hence atmosphere-ocean interactions are of particular importance. The coupled model simulates a stable equilibrium climate without the need for any artificial adjustments of the fluxes between the ocean and the atmosphere. We compare the simulated fields of sea surface temperature, surface wind, ocean currents and circulations, rainfall distribution, and evaporation against observations. While differences between simulations and observations are noted and will be the subject for further investigations, the coupled model succeeds in simulating the main features of the regional climate over the Maritime Continent including the seasonal north-south progression of the rainfall maxima and associated reversal of the direction of the ocean currents and circulation driven by the surface wind. Our future research will focus on addressing some of the deficiencies in the coupled model (e.g. wet bias in rainfall and cold biases in sea surface temperature) and on investigating the predictability of the regional climate system.

Keywords: Air-sea interactions, regional atmosphere-ocean coupled model, climate variability, Southeast Asia monsoon

1. Introduction and Background

The maritime continent is highly complex with relatively large ocean coverage and chains of islands that cover a range of different sizes. One significant challenge in simulating rainfall over the region is how to represent accurately the atmosphere-ocean-land interactions for a range of spatial and temporal scales. Due to the large ocean areas, air–sea feedbacks processes will be important in modeling the climate of this region, since the local sea surface temperature (SST) is among the major factors that shape rainfall variability across the Maritime Continent, and is in turn shaped by heat and moisture fluxes. Uncoupled atmospheric models prescribe spatially and temporally interpolated SST fields, while uncoupled ocean models prescribe ocean surface wind stress and heat and moisture fluxes. The latter ones are calculated either using bulk formulae or, more recently, taken from community atmospheric datasets such as the NCEP reanalysis (Kalnay et al., 1996). However, such models configurations ignore the dynamical interactions that occur at the atmosphere-ocean boundary. An integrated or coupled atmosphere-ocean model should be capable of simulating more realistic dynamics close to the ocean surface, where atmosphere-ocean exchanges take place, at a high frequency determined by the nature of the coupling.

Several research groups were successful in coupling regional models of the atmosphere and the ocean in the last decade. Early progress in building a regional coupled model was made within the Baltic Sea Experiment. Gustafsson et al. (1998) coupled a high-resolution atmospheric model to a lower solution ice–ocean model with the purpose of improving accuracy of weather forecasting over the Baltic Sea. Hagedorn et al. (2000) coupled the Max Plank Institute (MPI) Regional Atmospheric Model (REMO) to the 3D Kiel ocean model over the same area. The accuracy of the SST simulated by the coupled model was improved, even without any flux correction. Schrum et al. (2003) coupled the same atmospheric model to the 3D Hamburg Ocean

Model. Their results showed that the coupled atmosphere–ocean simulations produced better results compared to the same atmospheric model simulations forced by prescribed SST.

Similar studies were carried over other European domains. Döscher et al. (2002) developed a regional coupled ocean–atmosphere–ice model (RCAO) with the aim of simulating regional coupled climate scenarios over northern Europe. In order to explicitly resolve the two-way interactions at the air-sea interface over the Mediterranean region, Somot et al. (2008) coupled the global atmospheric model ARPEGE with the regional ocean model OPAMED. Since the ARPEGE spatial resolution was locally increased over the region of interest, the simulations are effectively comparable to a regional model simulation. Their results showed that the climate change signal in the coupled model simulations was generally more intense over large areas, with wetter winters over northern Europe and drier summers over Southern and Eastern Europe. The better simulated Mediterranean SST appears to be one of the factors responsible for such differences. In a similar study, RegCM3-MITgcm coupled model has been employed over the Mediterranean area (Artale et al., 2009). The model is able to capture the inter-annual variability of SST and also correctly describes the daily evolution of SST under strong air-sea interaction conditions. On the other hand, coupled models have been used to study extreme weather events. Loglisci et al. (2004) applied their coupled model to study the effect of a "bora" wind event on the dynamics and thermodynamics of the Adriatic Sea. They found that accurate heat flux from the sea surface is necessary for better representation of air–sea interactions associated with this high wind event, and for improved simulations of SSTs response. Pullen et al. (2006) developed a regional coupled system comprising the Navy Coastal Ocean Model (NCOM) coupled to the Coupled Ocean–Atmosphere Mesoscale Prediction System (COAMPS) in the same region. They focused on the effects of fine-resolution SST on air properties, in particular during the course of a

85 "bora" wind event. They found that the simulated SST after such event had a stabilizing effect on
86 the atmosphere, thus reducing atmospheric boundary layer.

87 Coupled models also were used for studying regional atmosphere-ocean interactions in
88 Atlantic and Pacific Oceans using basin-scale models. Huang et al. (2004) applied a regional
89 coupling strategy in a global coupled atmosphere–ocean GCM, where active air–sea coupling is
90 allowed only in the Atlantic Ocean basin. This study was able to isolate the effects of local
91 feedbacks on the resulting mean SST fields. Xie et al. (2007) constructed the regional
92 atmosphere–ocean coupled system (iROAM) which couples a regional atmospheric model
93 (iRAM) to a basin-scale ocean model in the Pacific, with interactive coupling permitted only in
94 the eastern half of the basin. The model was specifically developed to reduce biases in the eastern
95 tropical Pacific climate, where many coupled GCMs face significant challenges. A major
96 advantage of iROAM is that by using a reasonably high resolution (0.5° in the atmosphere and
97 ocean) compared to most coupled GCMs, it can effectively explore the role of local air–sea
98 feedbacks arising from mesoscale ocean processes and land topography while allowing significant
99 internal coupled variability free from the prescribed lateral boundary conditions.

100 Within Asian domains, Aldrian et al. (2005) developed an advanced high-resolution
101 coupled models consisting of REMO atmospheric model and a global MPI ocean model to study
102 the effect of air–sea coupling on Indonesian rainfall. Ratnam et al. (2008) coupled the regional
103 atmospheric model RegCM3 with the regional ocean model POM over the Indian Ocean and
104 found that the coupling considerably improved the simulation of the Indian monsoon rain band
105 both over the ocean and land. A regional coupled model also has been shown to be useful in
106 simulating the East Asia summer monsoon (Ren and Qian 2005) despite the presence a cold drift

in SST in their model. Li and Zhou (2010) used a coupled model RegCM3-HYCOM, to improve the rainfall simulation of the East Asian monsoon.

In contrast to the coupling studies in abovementioned maritime continents, fewer coupled regional atmosphere-ocean modeling studies have been carried over the Southeast Asian monsoon region, a region where a relatively shallow ocean occupies a significant fraction of the area and hence atmosphere-ocean interactions are of particular importance. This domain comprises the South China Sea (SCS) and its through-flow (SCSTF) and the Indonesian through-flow (ITF), the latter one constituting the major conduit of volume and property transports (heat, salinity, nutrients) from the Western Pacific to the Eastern Indian oceans (Figure 1). Most importantly, the ITF transfers coupled modes of climate variability, such as El Nino-Southern Oscillation (ENSO). The SCSTF and especially the ITF are subdivided into many pathways through both wide and narrow straits separated by the numerous islands of the Indonesian Archipelago. For a review of the ITF see Gordon (2005). Surface heat and moisture fluxes are especially important for the SCS which gains heat from the atmosphere at a rate in the range 20 - 50 W/m^2 per year and is also a recipient of heavy rainfall with an annual mean value of 0.2 ~ 0.3 Sv (1 Sv=10^6 m^3/s) over the entire basin. On the long time average this heat and freshwater gain is balanced by horizontal advection by the mean circulation. The cold, salty water of the western tropical Pacific entering through the Luzon strait in the northern SCS is transformed into warm, fresh water exiting from the southern Mindoro and Karimata straits. For a review of the SCS properties, see Qu et al. (2009). In a word, this complex geometry, together with equally complex atmosphere-ocean interactions, makes the modeling of the climate in this region a very challenging task.

2. Regional Atmospheric Model: RegCM3

Regional Climate Model (RegCM) was originally developed at the National Center for Atmospheric Research (NCAR) and is now maintained by the International Center for Theoretical Physics (ICTP). It is a three-dimensional, hydrostatic, compressible, primitive equation, σ-coordinate regional climate model. The dynamical core of RegCM Version 3 (RegCM3) is based on the hydrostatic version of the Pennsylvania State University / NCAR Mesoscale Model Version 5 (MM5; Grell et al. 1994) and employs NCAR's Community Climate Model Version 3 (CCM3) atmospheric radiative transfer scheme (described in Kiehl et al. 1996). Planetary boundary layer dynamics follow the non-local formulation of Holtslag et al. (1990; described in Giorgi et al. 1993a). Ocean surface fluxes are handled by Zeng's bulk aerodynamic ocean flux parameterization scheme (Zeng et al. 1998). The Subgrid Explicit Moisture Scheme (SUBEX) is used to handle large-scale, resolvable, non-convective clouds and precipitation (Pal et al. 2000). Finally, three different convective parameterization schemes are available for representation of non-resolvable rainfall processes (Giorgi et al. 1993b): Kuo (Anthes 1977), Grell (Grell 1993) with Fritsch-Chappell (Fritsch and Chappell 1980) or Arakawa-Schubert (Grell et al. 1994) closures, and Emanuel (Emanuel 1991; Emanuel and Zivkovic-Rothman 1999). Further details of the developments and description of RegCM3 are available in Pal et al. (2007).

To represent the land surface physics, RegCM3 is coupled to the land surface scheme Biosphere Atmosphere Transfer Scheme Version 1e (BATS1e; described in Dickinson et al. 1993). BATS1e uses a one-layer canopy with two soil layers and one snow layer to perform eight major tasks, including: calculation of soil, snow or sea-ice temperature in response to net surface heating, calculation of soil moisture, evaporation and surface and groundwater runoff, calculation

151 of the plant water budget, including foliage and stem water storage, intercepted precipitation and
152 transpiration, and calculation of foliage temperature in response to energy-balance requirements
153 and consequent fluxes from the foliage to canopy air (Dickinson et al. 1993). Additional
154 modifications have been made to BATS1e to account for the subgrid variability of topography and
155 land cover as described in Giorgi et al. (2003).

156 Winter et al. (2009) coupled RegCM3 to an additional land surface scheme – the
157 Integrated Biosphere Simulator (IBIS; described in Foley et al. 1996). IBIS uses a hierarchical,
158 modular structure to integrate a variety of terrestrial ecosystem phenomena. IBIS contains four
159 modules, operating at different time steps, and includes a two-layer canopy with six soil layers
160 and three snow layers. The four modules simulate processes associated with the land surface
161 (surface energy, water, carbon dioxide and momentum balance), vegetation phenology (winter-
162 deciduous and drought-deciduous behavior of specific plant types in relation to seasonal climatic
163 conditions), carbon balance (annual carbon balance as a function of gross photosynthesis,
164 maintenance respiration and growth respiration), and vegetation dynamics (time-dependent
165 changes in vegetation cover resulting from changes in net primary productivity, carbon allocation,
166 biomass growth, mortality and biomass turnover for each plant functional type) (Foley et al.
167 1996).

168

169 **3. Regional Ocean Model: FVCOM**

170 FVCOM is a three dimensional, free surface, primitive equation, finite volume coastal
171 ocean model, originally developed by Chen et al. (2003). The model adopts a non-overlapping
172 unstructured (triangular) grid and finite volume method. The unstructured grid combines the

advantages of finite-element methods for geometric flexibility and finite-difference methods for computational efficiency. FVCOM solves the momentum and thermodynamic equations using a second order finite-volume flux discrete scheme that ensures mass conservation on the individual control volumes and the entire computational domain (Chen et al., 2006a,b). The Mellor and Yamada level 2.5 turbulent closure scheme is used for vertical eddy viscosity and diffusivity (Mellor and Yamada, 1982) and the Smagorinsky turbulence closure for horizontal diffusivity (Smagorinsky, 1963). The heat fluxes are assumed to occur at the ocean surface and the short wave radiation penetrated into the water column is approximated following Simpson and Dickey (1981). For details of FVCOM see http://fvcom.smast.umassd.edu/FVCOM/index.html.

In order to better represent the oceanic processes in the Southeast Asian region, the flexible unstructured grid is capable of designing a model domain with varied resolutions according to its complex geometry and topography. Our model domain covers the entire SCS, the western Pacific and the eastern Indian Ocean (Figure 3), with two open boundaries at the Pacific Ocean and the Indian Ocean respectively. This regional domain with open boundaries is chose to be large enough to prevent possible boundary effects, such as spurious wave reflection, from affecting the interior circulation. The grid contains 67,716 non-overlapping triangular cells and 34,985 nodes. The sigma coordinate is used in the vertical and is configured with 31 layers (finer at surface and coarser at depth), which provides a vertical resolution of <1 m near surface on the shelf, and about 10 m in the open ocean. The water depth at each grid point is interpolated from ETOPO5 (Figure 1). The horizontal resolution is ~10 km along the coast of the islands of the Indonesian Archipelago, ~50 km in the central SCS and ~200 km along the open boundaries.

For ocean-only simulations, such as during the spin-up phase, FVCOM is embedded with one way coupling in the global ocean MITgcm (Hill and Marshall, 1995; Marshall et al., 1997)

196 which is a component of the MIT Integrated Earth System Model. The latter one comprises the
197 ocean GCM, a primitive equation, three-dimensional model with the resolution of $2.5^{o}\times2^{o}$ and 22
198 vertical z-levels (layer thickness ranging from 10 m to 765 m). It includes a prognostic carbon
199 model. The atmosphere is represented by a statistical-dynamical two-dimensional (zonally
200 averaged) model with the resolution of 4^{o} and 11 vertical z-levels. Land, sea-ice and an active
201 chemistry model are also included. Flux adjustment is also used by restoring the SST to
202 observations. A "spreading" technique is used for the two-dimensional air-sea heat flux to
203 reconstruct the longitudinal dependence, i.e. dQ/dT*delta(T), where Q, latitude-dependent Q(y)
204 only, is the modeled calculated heat flux, and delta(T) is the difference of local temperature from
205 the zonal mean. Four decade simulations (60s-70s-80s-90s) are available from the MITgcm with
206 the full fields of currents, temperature, salinity and sea level. The atmospheric model provides the
207 surface heat and moisture fluxes. The wind stress however is given by the NCEP reanalysis with
208 6-hourly date for the entire period 1948-2000. The complex spin-up procedure of the MITgcm can
209 be found in http://mitgcm.org/public/r2_manual/latest/.

210

211 **4. Coupling of RegCM3 and FVCOM**

212 Here we developed a regional coupled atmosphere–ocean model in order to investigate the
213 climate over the Maritime Continent. The coupled model is developed using RegCM3 as the
214 atmospheric component and FVCOM as the oceanic component. The two models are coupled
215 using the OASIS3 software (http://www.cerfacs.fr/globc/software/oasis/oasis.html), which allows
216 flexible coupling for different model configurations and is suitable to run on massively parallel
217 computers.

In order to keep synchronization of RegCM3 and FVCOM, the two models are integrated forward simultaneously and OASIS3 interpolates and transfers the coupling fields of different resolution from the source grid to the target gird at a specified interval. At run time, RegCM3 and FVCOM are respectively driven by lateral boundary forcing. In FVCOM, lateral forcing includes SSH, temperature, and salinity along the open boundaries which are interpolated from simulations of the MITgcm. In RegCM3, the lateral forcing includes temperature, winds, relative humidity along the boundaries, interpolated from the European Centre for Medium-range Weather Forecasts (ECMWF) 40-year Re-Analysis (ERA40) dataset (Uppala et al. 2005). The coupling fields at the atmosphere-ocean interface were calculated in each model and exchanged through the coupler, that is, RegCM3 supplies the solar heat fluxes, latent heat flux, sensible heat flux, surface wind to FVCOM, and FVCOM provides SST for RegCM3. The timing of the exchange is shown in Figure 2. While at each time step the coupler is automatically requesting the coupling fields from the individual model, the exchange is actually taken place at every 6 hours, which is the same frequency at which lateral boundary conditions are provided to the atmospheric model. The details of the coupling process are described in the Appendix.

5. Results of Simulations using the Coupled Model

In order to investigate the decadal variability of climate over the Southeast Asian monsoon region (Figure 1), the RegCM3-FVCOM coupled model was integrated for from 1960-1980 and the results are validated with observations. The first decade simulation (60s) is for model spin-up and the results of the second decade (70s) are summarized and presented.

240 *5.1 Model spin-up (60s):*

241 The coupled model was first spun up from 1960 to 1969. For RegCM3, the SST is
242 initialized with GISST data and then updated every 6 hours by SST obtained from FVCOM.
243 FVCOM started from rest condition with initial temperature and salinity from the MITgcm
244 simulation which is the first weekly average field of 1960. Figure 4 shows such the initial
245 condition for SST with the MITgcm resolution ($2.5^o \times 2^o$) evident. The temperature (salinity) at the
246 boundaries is relaxed to the temperature (salinity) of the MITgcm simulation. Heat fluxes were
247 updated every 6 hours from RegCM3. To establish a reasonable atmosphere-ocean interface
248 thermal structure a flux correction is used during the model spin-up for the decade of the 60s.
249 Specifically, the SST is relaxed towards the SODA SST analysis (Carton et. al 2000a,b) with a
250 depth dependent nudging factor, ranging from 0.2 s^{-1} in shallow water and decreasing to 0.001 s^{-1}
251 in the open ocean. Thus in the open ocean the flux correction is negligible and the RegCM3 heat
252 fluxes dominate. In shallow water the flux correction dominates to keep the ocean model from
253 drifting from the climatology of the 60s. Furthermore, to obtain a stable reversal monsoon
254 circulation, sea level along the open boundaries at the Pacific and Indian Oceans is forced
255 perpetually by 10-year averages of weekly SSHA simulation from the MITgcm, and the surface
256 wind is gradually ramped up and updated every 6 hours from RegCM3.

257

258 *5.2 Results of the 70s:*

259 The simulation of the 70s was restarted from the model conditions saved at the end of the
260 60s. The model configuration of the 70s is the basically same as of the 60s except two changes.

First, differently from the spin-up phase, no flux correction is used in the simulation of the 70s, hence in FVCOM relaxation of the SST to the observations is turned off. Second, the sea level at open boundaries is driven by real time SSHA of the 70s.

The Southeast Asian monsoon circulation, especially in the South China Sea, is driven by surface wind and boundary sea level pressure gradient. Figure 5 show decadal average (70s) surface circulations for winter (DJF) and summer (JJA) seasons. The coupled model successfully reproduces the seasonal reversal of the SCSTF associated with the seasonality of the Southeast Asian monsoon, North-Eastern in winter and South-Western in summer (Figure 6, also see Qu, 2000). Figures 7a-b show 10-year time series of domain average wind from RegCM3 and surface eddy kinetic energy (EKE) from FVCOM. The wind speed clearly shows two peaks in each annual cycle associated with the winter northeast monsoon and the summer southwest monsoon. The surface EKE shows a very stable annual cycle throughout the 10-year simulation and is highly correlated with the wind fluctuation, which implies the strong monsoon-driven southwestward flow in winter and northeastward flow in summer (Figure 5). Similarly, the domain average net heat flux also shows a clear cyclicity (Figure 7c). There are two maxima occurred in summer when the incidence of the solar radiation is perpendicular to the earth equator due to earth revolution. Since the SST relaxation is turned off, the ocean SST in the 70s simulation is mainly driven by the heat fluxes as evident from Figure 7d.

5.3 Comparison with observations:

To assess the ability of the coupled model, here we compared the model results with reanalysis and observations. Figure 8 compares the model simulations of SST, the SODA SST

283 reanalysis and their difference. The overall SST patterns show important similarities, with a band
284 of cold Pacific water protruding into the northern SCS and a band of warm water over the
285 Indonesian archipelago and the ITF in (boreal) winter. The SST pattern is reversed in summer.
286 However, the model SST is overall colder than SODA SST by 2 to 4 degrees (Fig. 8e-f), except
287 for the southern coast of China where the model SST is warmer than SODA SST in winter. We
288 remind that the initial condition for the coupled simulation represents the realistic SST at the end
289 of the 60s as in the spin-up phase the SST is relaxed to the SODA field. Therefore, during the
290 coupled simulation without the flux correction the ocean SST drifts away from the SODA
291 reanalysis producing a colder ocean. There are many possible reasons for this discrepancy, the
292 most plausible one being that the water masses continuously prescribed at the open boundaries
293 from the MITgcm do not provide a correct distribution of the water masses. In fact, Figure 8e-f
294 shows consistently rather colder waters all along the open model boundaries with respect to the
295 SODA reanalysis, both in winter and summer. This is particularly true for the entire western
296 Pacific and the Eastern Indian oceans in summer. As the major advective pathways are from the
297 Pacific to the Indian both through the SCSTF and the ITF, over 10 years the advection of rather
298 colder waters would affect the entire interior of the domain.

299 Figure 9 compares the seasonal precipitation of model simulation with TRMM
300 observations. In winter (DJF), the simulation is able to reproduce the basic climatology over the
301 domain, but with more precipitation over the maritime continent mountainous regions and less
302 precipitation over some oceanic areas of northern hemisphere. In summer (JJA), a systematic
303 overestimation of precipitation occurs in the northern hemisphere and underestimation is found in
304 the southern part of domain, associated with the passages of rain belts. Station-based comparisons
305 are showed in Figure 10. It can be seen that the model capture the annual cycles of precipitation at

306 Hong Kong and Darwin, with slightly more precipitation in dry season and obviously more
307 precipitation in wet season, suggesting that the extent of overestimation tends to relate the
308 movement of rain belts. Observed rainfall values highlight small differences at Singapore in each
309 month and similar characteristic is seen in the model simulation, but the somewhat higher values
310 from Oct. to Dec. in observation and lower values from Jun. to Aug. in simulation are actually
311 different enough to degrade our comparison. In general, the model can reproduce reasonably well
312 observed pattern of precipitation, despite it seemingly produces too much precipitation at the
313 monsoon rain belt, especially over the mountainous regions. These biases may be due to the
314 deficiency of the coupled model in producing more convective precipitation.

315 We also compare the simulated evaporation against the available observational TRMM
316 datasets (Figure 11). Generally evaporation is larger in cold season than in warm season over the
317 air-sea interface due to strong wind which is successfully captured in our model simulations.
318 Statistically discrepancies between simulations and observations are that the model exhibits
319 positive anomalies over the air-sea interface in both winter and summer, which may be one of the
320 reasons for the overestimation of precipitation.

321

322 **6. Discussion, Summary, and Future Research**

323 In order to investigate the regional climate over the Maritime Continent, this study
324 presents a newly-developed regional atmosphere-ocean coupled model. The coupled model adopts
325 RegCM3 as the atmospheric component and FVCOM as the oceanic component, using the
326 OASIS3 as the coupler. RegCM3 includes several options for representing important processes
327 such as moist convection and land surface physics. FVCOM features a flexible unstructured grid

328 that can match the complex geometries of the lands and the system of islands comprised in the
329 region as well as its complex topography. To keep synchronization of RegCM3 and FVCOM, the
330 two models are integrated forward simultaneously. At run time, RegCM3 and FVCOM are
331 respectively driven by lateral boundary forcing and OASIS3 interpolates and transfers the
332 coupling fields of different resolution between the two models. RegCM3 supplies the solar heat
333 fluxes, latent heat flux, sensible heat flux, surface wind to FVCOM, while FVCOM provides SST
334 for RegCM3.

335 The coupled model is developed and tested over the Southeast Asian Maritime Continent,
336 a region where a relatively shallow ocean occupies a significant fraction of the area and hence
337 atmosphere-ocean interactions are of particular importance. The coupled model simulates a stable
338 equilibrium climate over a decade (1970-1980) without the need for any artificial adjustments of
339 the fluxes between the ocean and the atmosphere. We compare the simulated fields of sea surface
340 temperature, surface wind, ocean currents and circulation, rainfall distribution, and evaporation
341 against observations. The coupled model reproduces an overall realistic pattern of SST, even
342 though colder than the SODA reanalysis, the major features of the monsoon circulation, as well as
343 rainfall and evaporation distributions over the region. The model results are in reasonable
344 agreement with the observed atmosphere/ocean climatology, suggesting that the coupled model
345 successfully captures the decadal variability of climate over this region. While differences
346 between simulations and observations are noted and will be the subject for further investigations,
347 the coupled model succeeds in simulating the main features of the regional climate over the
348 Maritime Continent including the seasonal north-south progression of the rainfall maxima and
349 associated reversal of the direction of the ocean currents and circulation driven by the surface
350 monsoons. The comparison with observations shows some differences over the mountainous

351 regions, especially for the rainfall simulation (Figure 9). These biases may be due to the
352 deficiency in the representation of clouds and moist convection. For the ocean component, the
353 discrepancies observed in the model SST, colder than the observed ones, may be due to an
354 incorrect representation of the water masses at the open ocean boundaries interpolated from the
355 MITgcm simulations. Our future research will focus on addressing some of the stated deficiencies
356 in the coupled model (e.g. wet bias in rainfall and cold biases in SST) and on investigating the
357 predictability of the regional climate system.

358

Appendix

The coupling process includes the following steps:

OASIS3 Configuration and Auxiliary Files:

OASIS3 needs configuration and auxiliary files configuring a particular coupled run, describing coupling and I/O field names and units, defining the grids of the models, containing the field coupling initial data values or restart data values, as well as a number of other auxiliary data files used in specific transformations. The configuration file *namecouple* contains all users' defined information necessary to configure a particular run, such as the number of models being coupled, the number of fields, coupling period, transformation and interpolation methods, etc. The text file *cf_name_table.txt* contains a list of standard names and associated units identified with an index. This information will be used by OASIS3 for its log messages to *cplout* file. In this study, we configured two component models (RegCM3 and FVCOM) and 5 coupling fields (SST, solar heat fluxes, non-solar heat fluxes, zonal wind and meridional wind).

Definition of Grid Data Files

Before running the coupled model, the coupler OASIS3 requires grid information of each component model which can be created as netCDF files by users. The grid data files to be created are *grids.nc*, *mask.nc* and *areas.nc*. *grids.nc* contains the component model grids, longitude and latitude. The model grids can be any type of mesh, structured or unstructured. In this study, the atmosphere model (RegCM3) used structured grid (rectangular grid) while the ocean model (FVCOM) used unstructured grid (triangular grid). *masks.nc* contains the masks of atmosphere

379 and ocean for each component model. *areas.nc* contains mesh surfaces for the component model
380 grids.

381 *Coupler Initialization*

382 The subroutine *inicma* initializes and defines the variables returned by the coupler (SST) and
383 given to the coupler (solar heat fluxes, non-solar heat fluxes, zonal wind, meridional wind).

384 *Sending the coupling fields:*

385 This process is executed by calling the *intocpl* subroutine. RegCM3 supplies the solar heat fluxes
386 (short-wave and long-wave fluxes), non-solar heat fluxes (latent and sensible heat fluxes), zonal
387 wind (10 m) and meridian wind (10 m) and FVCOM supplies ocean SST to the coupler. While
388 this subroutine is called by each component model at each time step, the sending is actually
389 performed only if the time obtained by adding the fields lag to the argument date corresponds to
390 the time at which it should be activated.

391 *Receiving the coupling fields:*

392 This process is executed by calling the *fromcpl* subroutine. RegCM3 obtains SST and FVCOM
393 obtains solar and non-solar heat fluxes, and wind stress from the coupler. Similarly, the receiving
394 action is actually performed at the specific time at which it should be activated.

395 *Transformations and Interpolations:*

396 Different transformations and interpolations are available in OASIS3 to adapt the coupling fields
397 from the source model grid to the target model grid. In this study, we performed a time
398 transformation on all coupling fields, that is, before sending to the coupler, the coupling fields

were averaged over the previous coupling period. The interpolation techniques are from the software of SCRIP (http://climate.acl.lanl.gov/software/SCRIP). A conservative remapping scheme is used for solar and non-solar heat flux fields, which keeps the context fields conserved over the area-integrated field. As for other fields (SST and wind stress), a method of distance-weighted average of nearest-neighbor point interpolation is used.

Coupling restart file

When restart, the coupling fields have to be read from the coupling restart file on their source grid. In our coupled model, the routine of *prism_put_restart_proto* writes restart fields at the beginning of every month. The restart file is named *flda.nc* for RegCM3 and *fldo.nc* for FVCOM.

Termination

All processes must terminate the coupling by calling *quitcpl* subroutine. This will ensure a proper termination of all processes in the coupled model communicator.

Acknowledgment

This study was supported by the Singapore National Research Foundation (NRF) through the Singapore-MIT Alliance for Research and Technology (SMART) and Center for Environmental Sensing and Monitoring (CENSAM) and by National Natural Science Foundation of China (NSFC).

References

Aldrian E, Sein D, Jacob D, Du¨menil Gates L, Podzun R, 2005: Modeling Indonesian rainfall with a coupled regional model. *Clim Dyn* 25:1–17

Anthes, R. A, 1977: A cumulus parameterization scheme utilizing a one-dimensional cloudmodel, *Mon. Wea. Rev.*, 105, 270-286.

Artale, V., Calmanti, S., and Carillo, A., et al., 2009: An atmosphere–ocean regional climate model for the Mediterranean area: assessment of a present climate simulation. *Clim Dyn*, doi 10.1007/s00382-009-0691-8

Carton, J.A., G. Chepurin, X. Cao, and B.S. Giese, 2000a: A Simple Ocean Data Assimilation analysis of the global upper ocean 1950-1995, Part 1: methodology, *J. Phys. Oceanogr.*, 30, 294-309.

Carton, J.A., G. Chepurin, and X. Cao, 2000b: A Simple Ocean Data Assimilation analysis of the global upper ocean 1950-1995 Part 2: results, *J. Phys. Oceanogr*., 30, 311-326.

Chen, C., H. Liu and R. C. Beardsley, 2003: An unstructured, finite-volume, three-dimensional, primitive equation ocean model: application to coastal ocean and estuaries. *J. Atmos. Oceanic Tech.*, 20, 159-186.

Chen, C., R.C. Beardsley, and G. Cowles, 2006a: An unstructured grid, finite-volume coastal ocean model-FVCOM user manual, School for Marine Science and Technology, University of Massachusetts Dartmouth, New Bedford, Second Edition. *Technical Report SMAST/UMASSD-06-0602*, 318pp.

Chen, C, R. C. Beardsley and G. Cowles, 2006b: An unstructured grid, finite-volume coastal ocean model (FVCOM) system. Special Issue entitled "Advance in Computational Oceanography", *Oceanography*, 19(1), 78-89.

Dickinson, R., A. Henderson-Sellers, and P. Kennedy, 1993: Biosphere Atmosphere Transfer Scheme (BATS) version 1e as coupled to the NCAR Community Climate Model, NCAR Technical Note NCAR/TN-387+STR, National Center for Atmospheric Research, Boulder, Colorado.

Döscher, R., U. Willén, C. Jones, A. Rutgersson, H. E. M. Meier, U. Hansson, and L. P. Graham, 2002: The development of the regional coupled ocean–atmosphere model RCAO. *Boreal Environ. Res.*, 7, 183–192.

443 Emanuel, K. A., 1991: A scheme for representing cumulus convection in large-scale models, *J. Atmos. Sci.*,
444 48(21), 2313-2335.

445 Emanuel, K. A., and M. Zivkovic-Rothman, 1999: Development and evaluation of a convection scheme for use
446 in climate models, *J. Atmos. Sci.*, 56, 1766-1782.

447 Foley, J. A., I. C. Prentice, N. Ramankutty, S. Levis, D. Pollard, S. Sitch, and A. Haxeltine, 1996: An integrated
448 biosphere model of land surface processes, terrestrial carbon balance, and vegetation dynamics, Global
449 Biogeochem. *Cycles*, 10(4), 603-628.

450 Fritsch, J. M., and C. F. Chappell, 1980: Numerical prediction of convectively driven mesoscale pressure
451 systems. Part 1: Convective parameterization, *J. Atmos. Sci.*, 37, 1722-1733.

452 Giorgi, F., M. R. Marinucci, and G. T. Bates, 1993a: Development of a second-generation regional climate
453 model (RegCM2). Part I: Boundary-layer and radiative transfer processes, *Mon. Wea. Rev.*, 121, 2794-
454 2813.

455 Giorgi, F., M. R. Marinucci, and G. T. Bates, 1993b: Development of a second-generation regional climate
456 model (RegCM2). Part II: Convective processes and assimilation of lateral boundary conditions, *Mon. Wea.*
457 *Rev.*, 121, 2814-2832.

458 Giorgi, F., R. Francisco, and J. S. Pal, 2003: Effects of a sub-grid scale topography and land use scheme on the
459 simulation of surface climate and hydrology. Part I: Effects of temperature and water vapour
460 disaggregation, *J. Hydrometeorol.*, 4, 317-333.

461 Gordon, et.al., 2005: Oceanography of the Indonesian seas and their through-flow. 18, 4, 14-27

462 Grell, G. A., 1993: Prognostic evaluation of assumptions used by cumulus parameterizations, *Mon. Wea. Rev.*,
463 121, 764-787.

464 Grell, G. A., J. Dudhia, and D. R. Stauffer, 1994: Description of the fifth generation Penn State/NCAR
465 Mesoscale Model (MM5), *Technical Report TN-398+STR*, National Center for Atmospheric Research,
466 Boulder, Colorado.

467 Gustafsson, N., L. Nyberg, and A. Omstedt, 1998: Coupling of a high-resolution atmospheric model and an
468 ocean model for the Baltic Sea. *Mon. Wea. Rev.*, 126, 2822–2846.

Hagedorn, R., A. Lehmann, and D. Jacob, 2000: A coupled high resolution atmosphere–ocean model for the BALTEX region. *Meteor. Z.*, 9, 7–20.

Hill, C. and J. Marshall, 1995: Application of a Parallel Navier-Stokes Model to Ocean Circulation in Parallel Computational Fluid Dynamics In Proceedings of Parallel Computational Fluid Dynamics: Implementations and Results Using Parallel Computers, 545-552.

Holtslag, A. A. M., E. I. F. de Bruijn, and H.-L. Pan, 1990: A high-resolution air mass transformation model for short-range weather forecasting, *Mon. Wea. Rev.*, 118, 1561-1575.

Huang, B., P. S. Schopf, and J. Shukla, 2004: Intrinsic ocean–atmosphere variability of the tropical Atlantic Ocean. *J. Climate*, 17, 2058–2077.

Kalnay, E., M.Kanamitsu et al., 1996: The NCEP/NCAR 40-year Reanalysis Project, *Bull.Amer.Meteor.Soc.*, 77,437-471

Kiehl, J. T., J. J. Hack, G. B. Bonan, B. A. Boville, B. P. Breigleb, D. L. Williamson, and P. J. Rasch, 1996: Description of the NCAR Community Climate Model (CCM3), *NCAR Technical Note TN-420+STR*, [Available online at: http://www.cgd.ucar.edu/cms/ccm3/TN-420/].

Li T, Zhou G Q., 2010, Preliminary results of a regional air-sea coupled model over East Asia. *Chinese Sci Bull*, 55, doi: 10.1007/s11434-010-0071-0

Loglisci, N., and Coauthors, 2004: Development of an atmosphere–ocean coupled model and its application over the Adriatic Sea during a severe weather event of bora wind. *J.Geophys. Res.*, 109, D01102, doi:10.1029/2003JD003956.

Marshall, J., C. Hill, L. Perelman, and A. Adcroft, 1997: Hydrostatic, quasi-hydrostatic, and nonhydrostatic ocean modeling. *J. Geophys. Res.*, 102(C3), 5733-5752.

Mellor, G. L. and T. Yamada (1982), Development of a turbulence closure model for geophysical fluid problem. *Rev. Geophys. Space Phys.*, 20, 851-875.

Pal, J. S., and Coauthors, 2007: Regional climate modeling for the developing world: The ICTP RegCM3 and RegCNET, *Bull. Am. Meteorol. Soc.*, 88, 1395-1409.

494 Pal, J. S., E. E. Small, and E. A. B. Eltahir, 2000: Simulation of regional-scale water and energy budgets:
495 Representation of subgrid cloud and precipitation processes within RegCM, *J. Geophys. Res. (Atmos.),*
496 105(D24), 579-594.

497 Pullen, J., J. D. Doyle, and R. P. Signell, 2006: Two-way air–sea coupling: A study of the Adriatic. *Mon. Wea.*
498 *Rev.*, 134, 1465–1483.

499 Qu, T. 2000: Upper-Layer Circulation in the South China Sea, *J.Phys.Oceanogr.*, 30, 1450-1460

500 Qu, T., Y.T.Song and T.Yamagata, 2009: An introduction to the South China Sea through-floe: its dynamics,
501 variability and application for climate, *Dyn.Atnos.Oceans*, 47, 3-14

502 Ratnam JV, Giorgi F, Kaginalkar A, Cozzini S, 2008: Simulation of the Indian monsoon using the RegCM3–
503 ROMS regional coupled model. *Clim Dyn*. doi:10.1007/s00382-008-0433-3

504 Ren, X., and Y. Qian, 2005: A coupled regional air–sea model, its performances and climate drift in simulation
505 of the east Asian summer monsoon in 1998. *Int. J. Climatol.*, 25, 679–692.

506 Schrum, C., U. Hübner, D. Jacob, and R. Podzun, 2003: A coupled atmosphere/ice/ocean model for the North
507 Sea and Baltic Sea. *Climate Dyn.*, 21, 131–141.

508 Simpson, J. J. and T. D. Dickey, 1981: Alternative parameterizations of downward irradiation and their
509 dynamical significance. *J. Phys. Oceanogr.*, 11, 876-882

510 Smagorinsky, J. (1963), General circulation experiments with the primitive equations, I. The basic experi-ment.
511 *Mon. Wea. Rev.*, 91, 99–164.

512 Somot S, Sevault F, De´que´ M, Cre´pon M, 2008: 21st Century climate change scenario for the Mediterranean
513 using a coupled atmosphere-ocean regional climate model. *Glob Planet Change* 63(2–3):112–126

514 Uppala, S. M., and Coauthors, 2005: The ERA-40 Re-Analysis, Q. J. R. Meteorol. Soc., 131, 2961-3012.
515 [Dataset available online at: http://www.ecmwf.int/research/era/do/get/era-40]. Valcke S, Redler R, 2006:
516 OASIS3 User guide. PRISM support initiative report no 4, 60 pp

517 Xie, S.-P., and Coauthors, 2007: A regional ocean–atmosphere model for eastern Pacific climate: Toward
518 reducing tropical biases. *J. Climate,* 20: 1504—1522, doi: 10.1175/JCLI4080.1

519 Zeng, X., M. Zhao, and R. E. Dickinson, 1998: Intercomparison of bulk aerodynamic algorithms for the
520 computation of sea surface fluxes using TOGA COARE and TAO data, *J. Climate.*, 11, 2628-2644.

521

522 **List of Figures**

549 Figure 11: Comparison of evaporation between model simulations (1970s average) and TRMM
550 data (average of 1998~2011). (a) Model winter average evaporation, (b) Model
551 summer average evaporation, (c) Observed winter average evaporation and (d)
552 Observed summer average evaporation.

553

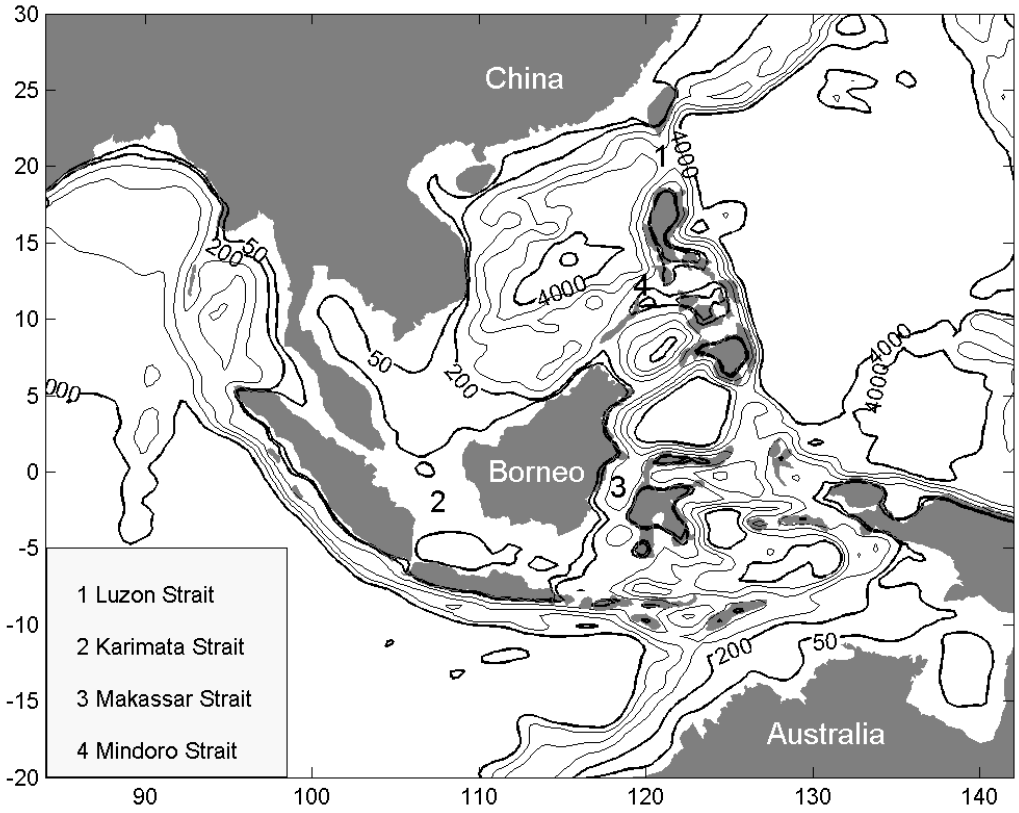

554

555 Figure 1: RegCM3 domain and bathymetry with the 50, 200 and 4000 m isobaths shown as
556 thicker lines, and 1000, 2000 and 3000 m isobaths shown as thin lines. The major straits are
557 marked.

558

559

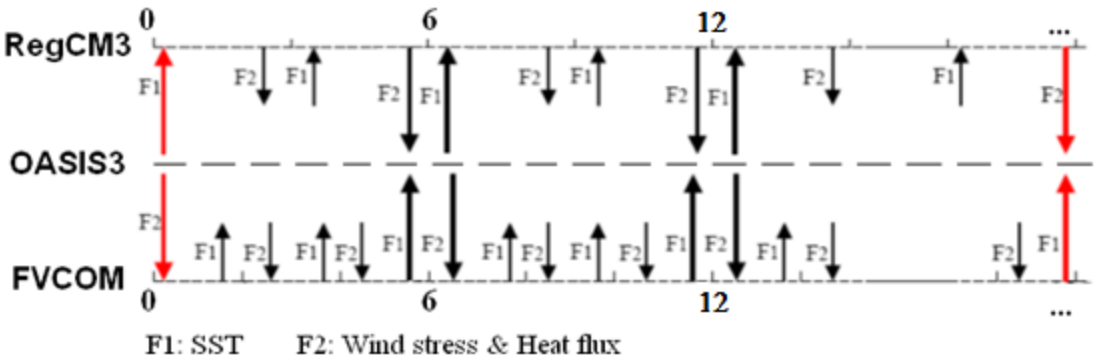

Figure 2: Schematic of RegCM3-OASIS3-FVCOM coupled model. The coupling fields (F1: SST; F2: wind and heat fluxes) are exchanged every 6 hours.

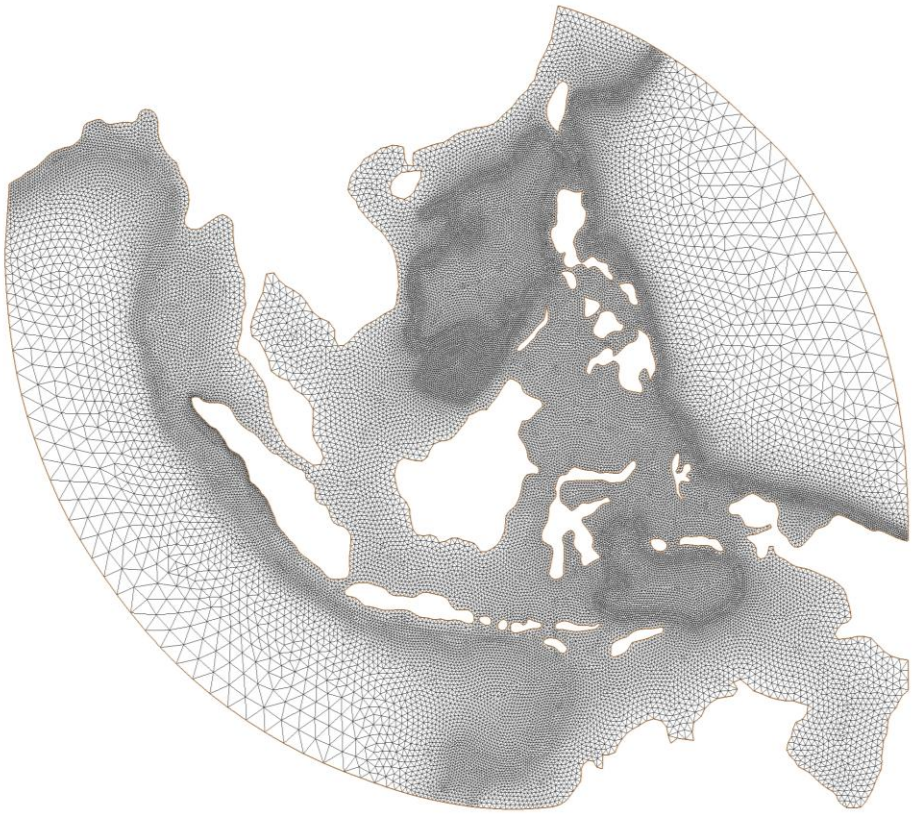

564

565 Figure 3: FVCOM unstructured grids which contain 67,716 non-overlapping triangular cells and
566 34,985 nodes.

567

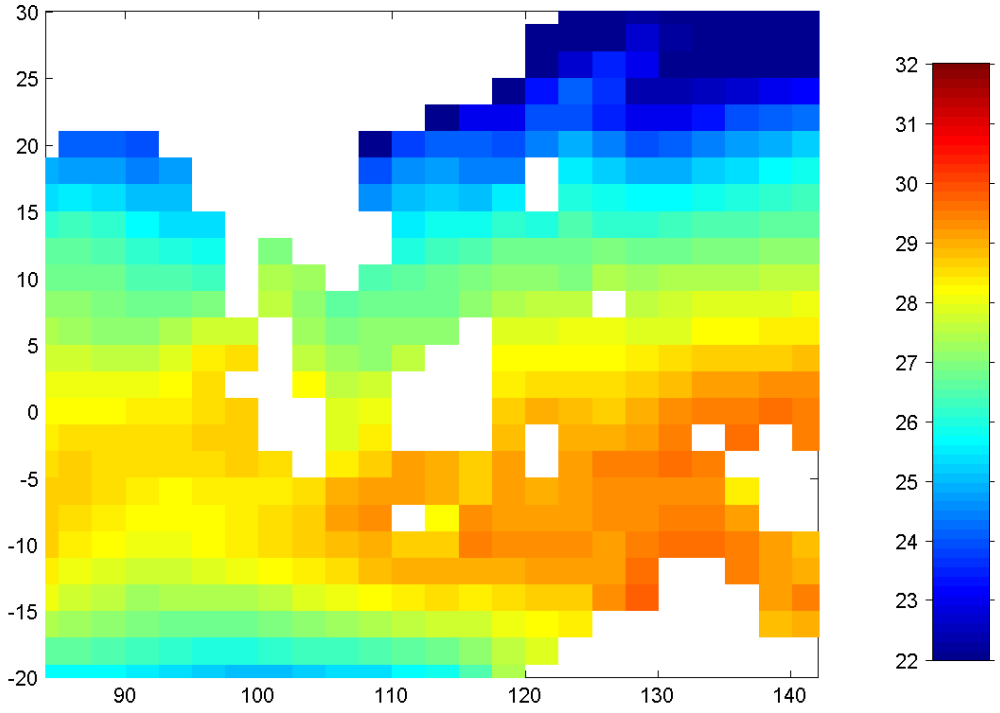

Figure 4: The weekly average of January 1st ~ 7th, 1960 from MITgcm simulations, which is used as initial SST in the coupled model. The MITgcm SST has resolution of 2.5°×2° and was interpolated to FVCOM grids.

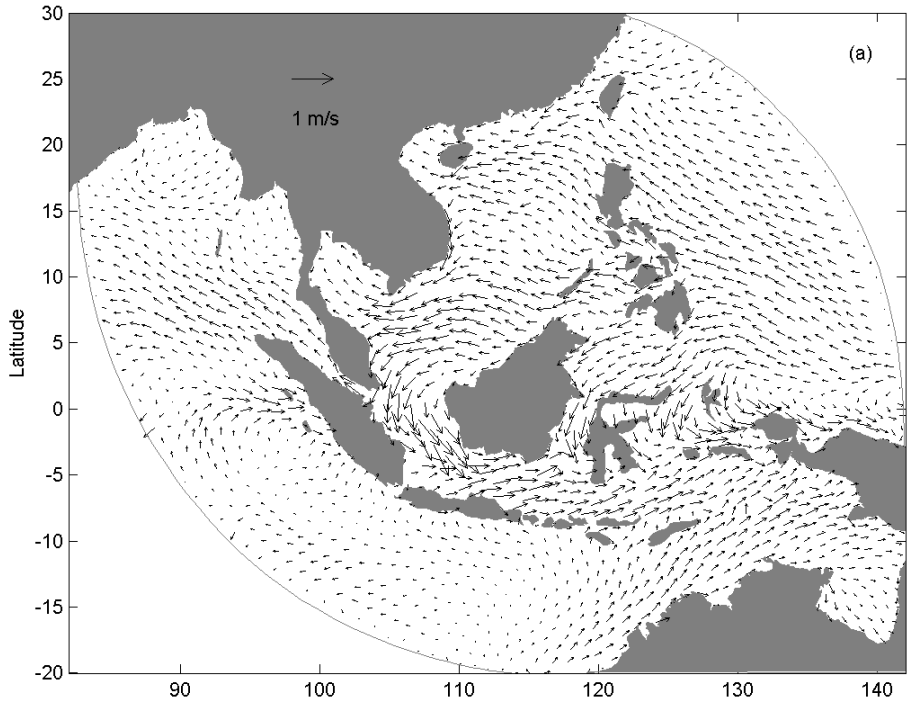

573

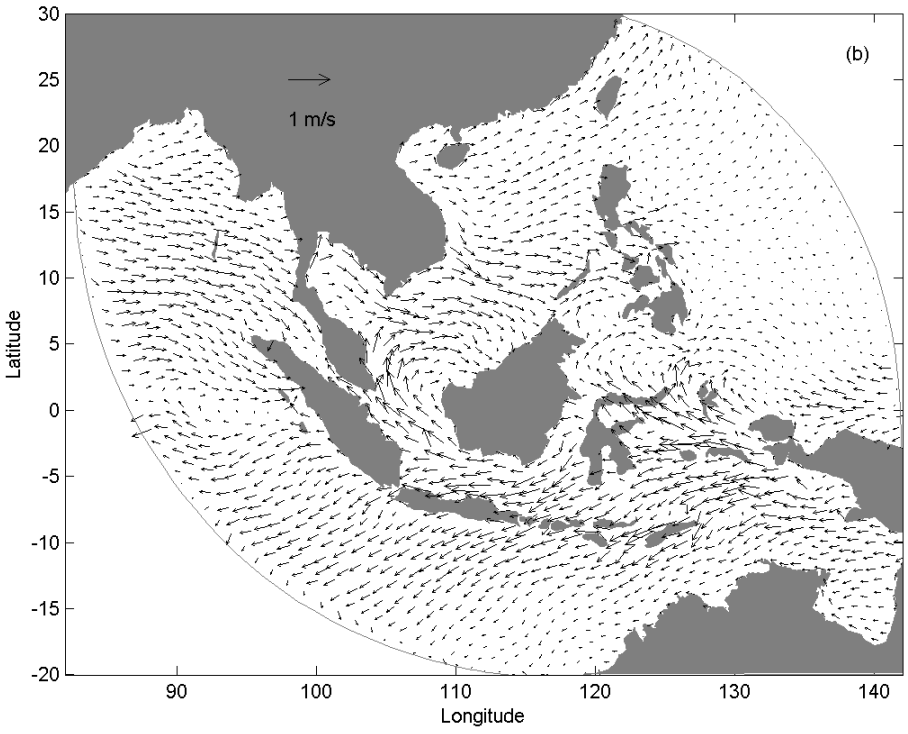

574

575 Figure 5: 10-year average surface circulations for (a) winter and (b) summer. The vectors shown
576 are extracted from FVCOM grid every 100 km.

577

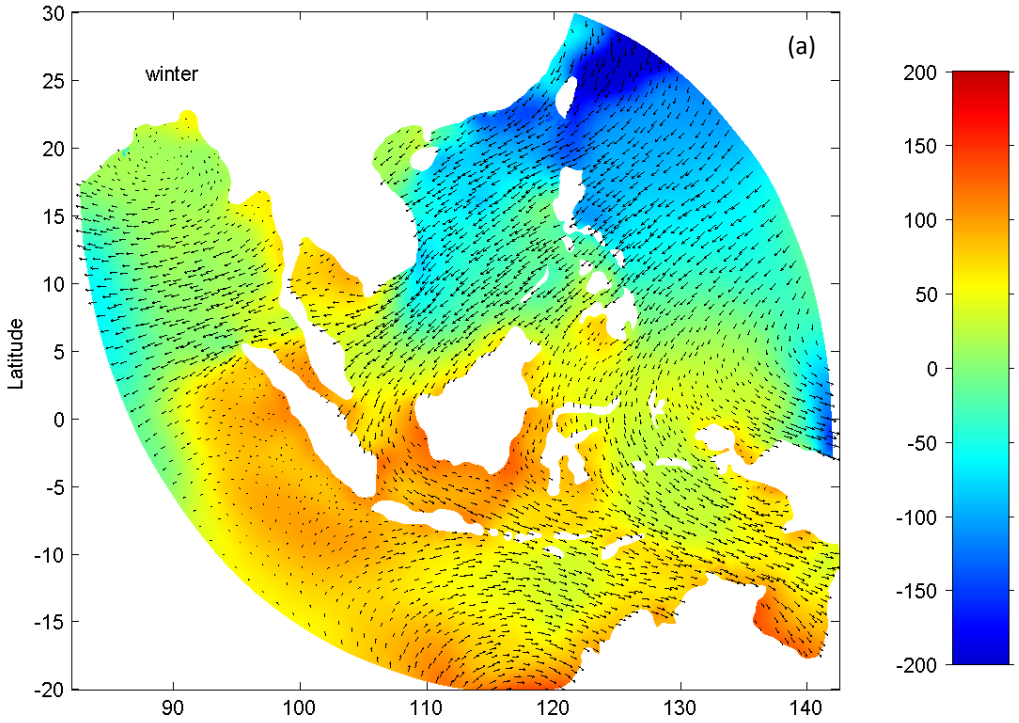

578

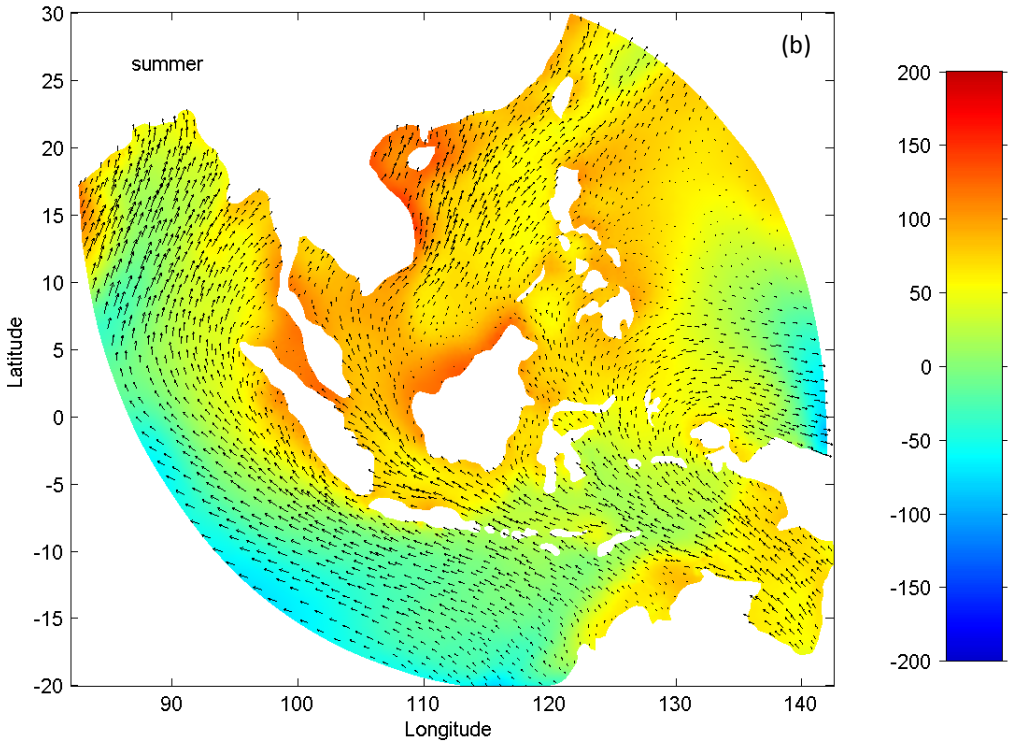

579 Figure 6: 10-year average net heat flux and wind speed for (a) winter and (b) summer. The wind
580 vectors shown are extracted from FVCOM grid every 50 km.

581

582

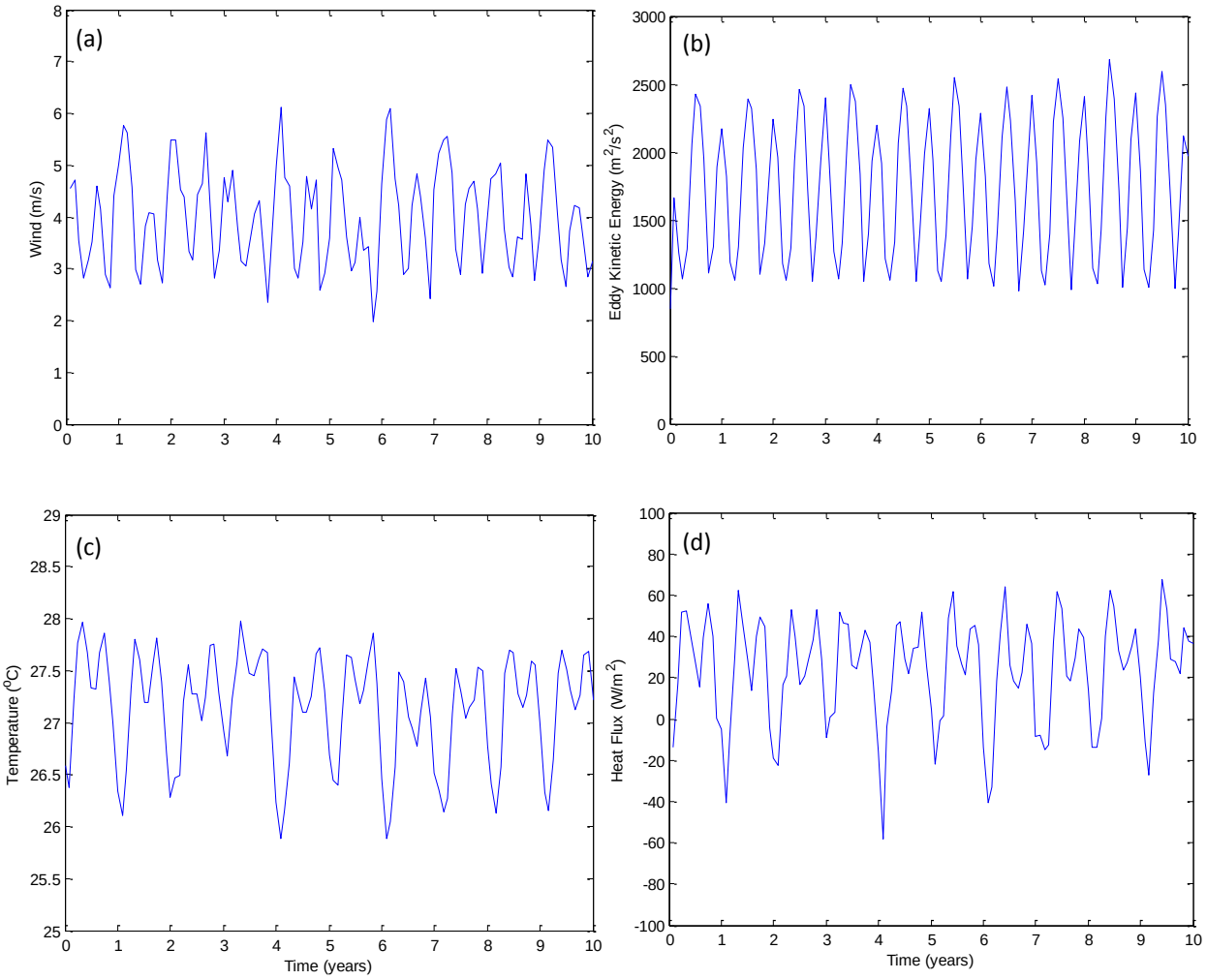

583

584 Figure 7: Time series (1970-1980) of domain average (a) wind speed, (b) eddy kinetic energy, (c)
585 SST and (d) net heat flux from 1970s simulations. Wind speed and net heat flux are calculated in
586 RegCM3, and eddy kinetic energy and SST are calculated in FVCOM.

587

588
589
590
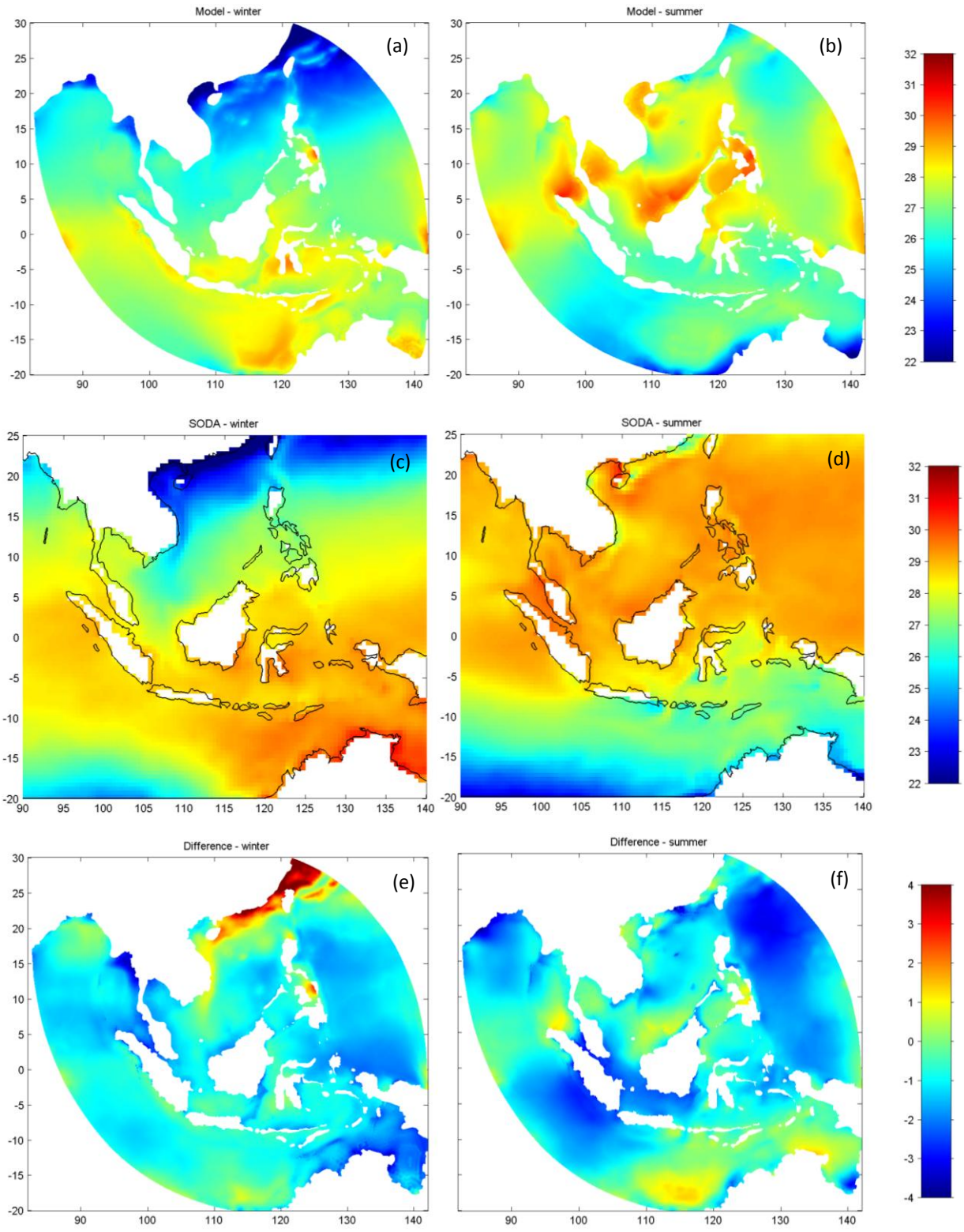

591 Figure 8: Comparison of model simulations of SST (a-b), SODA SST reanalysis (c-d). The
592 differences (e-f) are calculated as (Model – SODA).

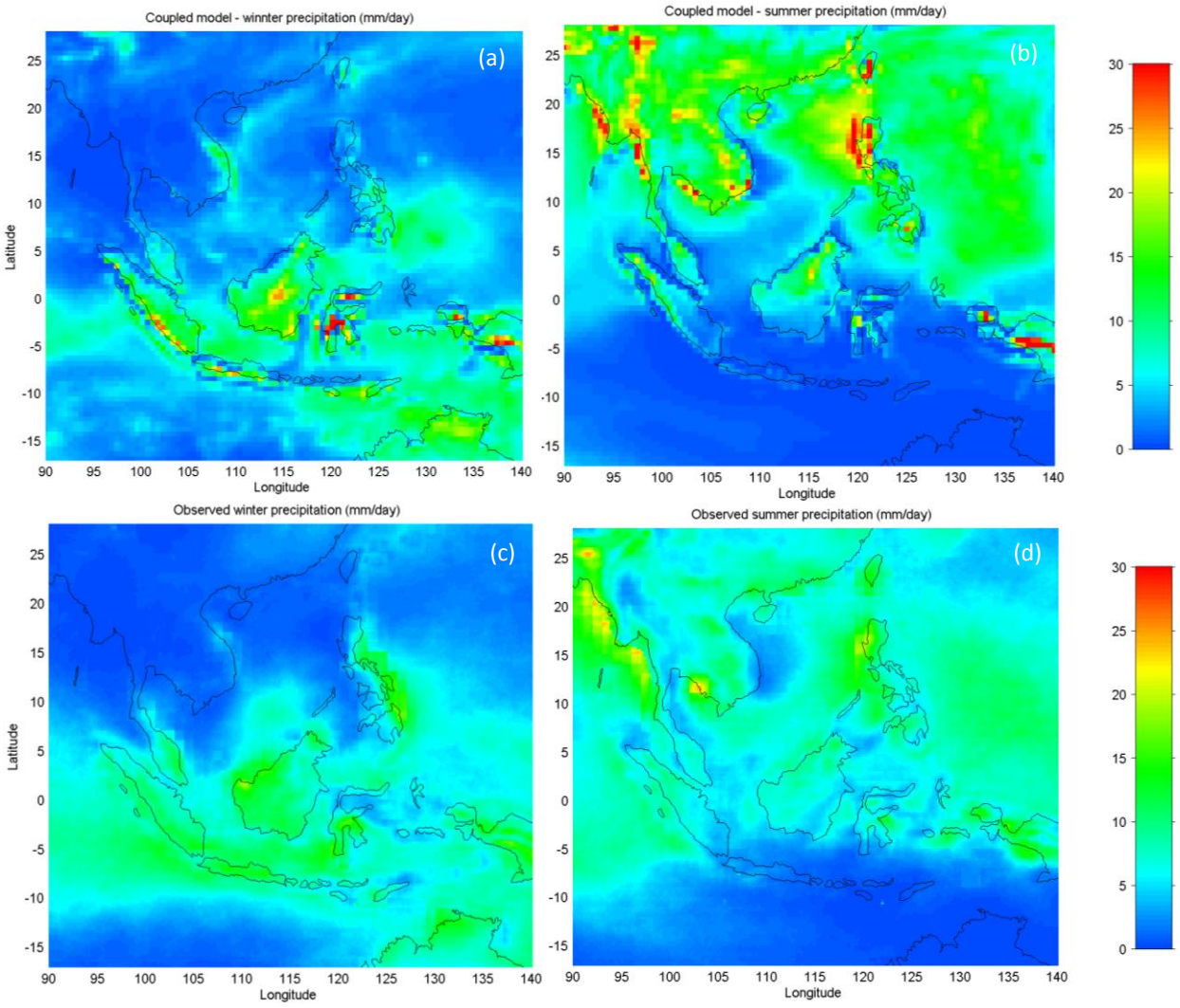

Figure 9: Comparison of precipitation between model simulations (1970s average) and TRMM data (average of 1998~2011). (a) Model winter average precipitation, (b) Model summer average precipitation, (c) Observed winter average precipitation and (d) Observed summer average precipitation.

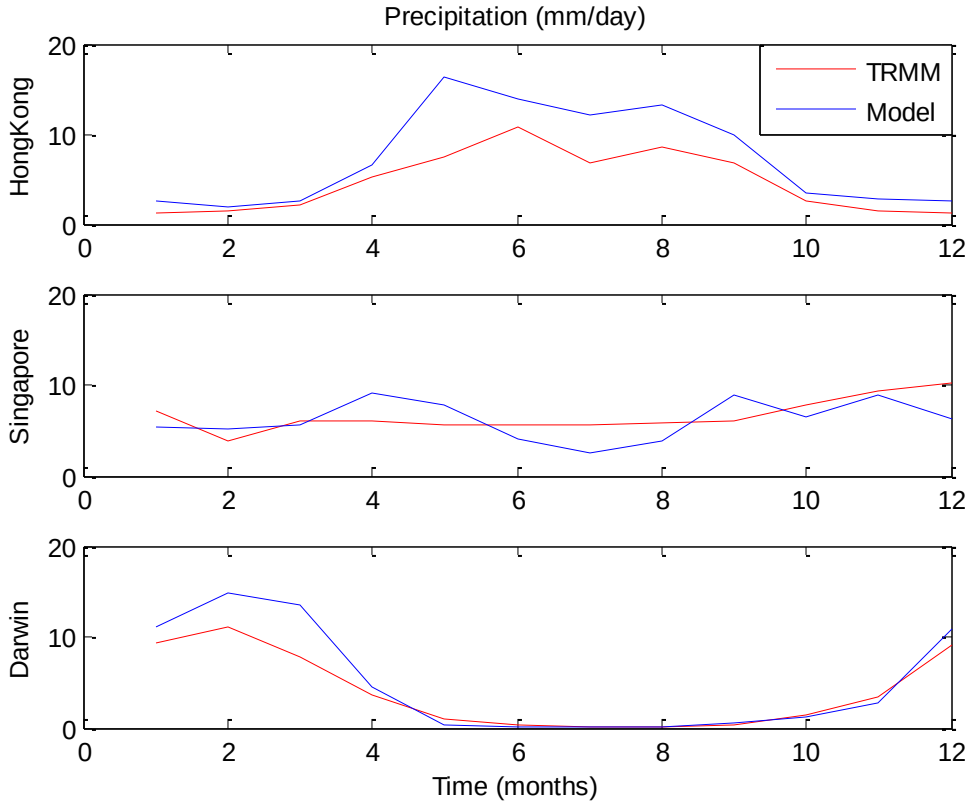

600

601 Figure 10: Comparison of annual cycle between observed and model precipitation at three
602 locations: Hong Kong, Singapore and Darwin. The observations and simulations are spatial
603 average within a $5^{o}\times5^{o}$ box centered at the three locations respectively.

604

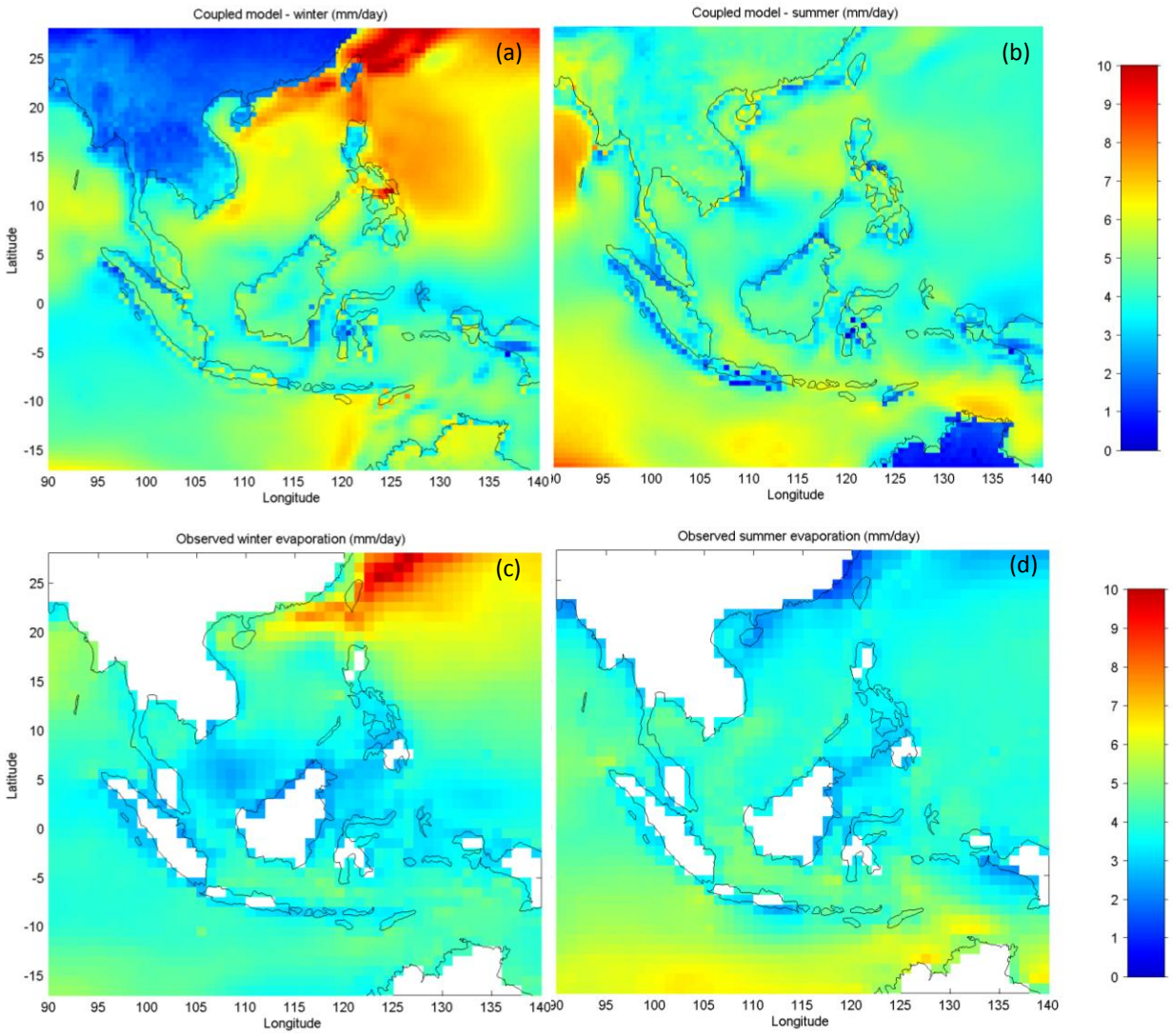

Figure 11: Comparison of evaporation between model simulations (1970s average) and TRMM data (average of 1998~2011). (a) Model winter average evaporation, (b) Model summer average evaporation, (c) Observed winter average evaporation and (d) Observed summer average evaporation.